Laboratory Investigation (2020) 100:606–618
https://doi.org/10.1038/s41374-019-0356-0

ARTICLE

Immunomodulator polyinosinic-polycytidylic acid enhances the inhibitory effect of 13-*cis*-retinoic acid on neuroblastoma through a TLR3-related immunogenic-apoptotic response

Hui-Ching Chuang[1,2] · Hung-Yu Lin[2,3] · Pei-Lin Liao[2,3] · Chao-Cheng Huang[4] · Li-Ling Lin[5] · Wen-Ming Hsu[6] · Jiin-Haur Chuang[2,3]

Received: 4 June 2019 / Revised: 18 October 2019 / Accepted: 3 November 2019 / Published online: 19 December 2019

Abstract

High-risk neuroblastoma is associated with low long-term survival rates due to recurrence or metastasis. Retinoids, including 13-cis-retinoic acid (13cRA), are commonly used for the treatment of high-risk neuroblastoma after myeloablative therapy; however, there are significant side effects and resistance rates. In this study, we demonstrated that 13cRA has a better antiproliferative effect in *MYCN*-amplified neuroblastoma cells than in *MYCN*-nonamplified neuroblastoma cells. In *MYCN*-amplified SK-N-DZ cells, 13cRA induced significant upregulation of toll-like receptor 3 (TLR3) and mitochondrial antiviral-signaling protein (MAVS) expression in a time-dependent manner. Furthermore, poly (I:C), a synthetic agonist of TLR3, effectively synergized with 13cRA to enhance antiproliferative effects through upregulation of the innate immune signaling and the mitochondrial stress response, leading to augmentation of the apoptotic response in 13cRA-responsive cancer cells. In addition, the 13cRA/poly (I:C) combination induced neural differentiation through activation of retinoic acid receptors beta (RAR-β), restoring expression of α-thalassemia/mental retardation syndrome X-linked (ATRX) protein, and inhibiting vessel formation, leading to retarded tumor growth in a mouse xenograft model. These results suggest that the combination of poly (I:C) and RA may provide synergistic therapeutic benefits for treatment of patients with high-risk neuroblastoma.

Introduction

Neuroblastoma is the most common extracranial neurogenic tumor occurring in children; while the long-term survival rate of high-risk neuroblastoma patients is <50% due to clinical heterogeneity and recurrent/metastatic disease [1–3]. For certain patients, a multidisciplinary treatment consisting of intensive induction and myeloablative chemotherapy followed by the treatment of the residual disease using differentiation therapy and immunotherapy is commonly recommended [3, 4].

Retinoids, including all-trans-retinoic acid (ATRA), 13-cis-retinoic acid (13cRA; Isotretinoin), and fenretinide (4-HPR), are vitamin A analogs, and have been used as cancer chemotherapeutic or chemopreventive agents due to their ability to induce cell differentiation, antiproliferation, and proapoptosis [5]. While both ATRA and 13cRA are commonly applied in therapy, 13cRA has exhibited more efficacy in the treatment of high-risk neuroblastoma after myeloablative therapy, significantly improving the 5-year overall survival rate of neuroblastoma patients [6].

Supplementary information The online version of this article (https://doi.org/10.1038/s41374-019-0356-0) contains supplementary material, which is available to authorized users.

✉ Jiin-Haur Chuang
jhchuang@cgmh.org.tw

1 Department of Otolaryngology, Kaohsiung Chang Gung Memorial Hospital and Chang Gung University College of Medicine, Kaohsiung, Taiwan

2 Mitochondrial Research Unit, Kaohsiung Chang Gung Memorial Hospital and Chang Gung University College of Medicine, Kaohsiung, Taiwan

3 Department of Pediatric surgery, Kaohsiung Chang Gung Memorial Hospital and Chang Gung University College of Medicine, Kaohsiung, Taiwan

4 Department of Pathology, Kaohsiung Chang Gung Memorial Hospital and Chang Gung University College of Medicine, Kaohsiung, Taiwan

5 Department of Molecular Medicine, University of Texas Health Science Center at San Antonio, San Antonio, TX, USA

6 Department of Surgery, National Taiwan University Hospital, National Taiwan University College of Medicine, Taipei, Taiwan

The development of strategies to improve resistance to retinoids and to address potential side effects of 13cRA in neuroblastoma patients are vital issues. As such, RA in combination with other designated compounds has been shown to regulate the functions of inflammation, cell proliferation, and differentiation statues, leading to increased treatment effectiveness [7, 8].

Retinoids activate transcription of RA-mediated genes by interacting with two nuclear hormone receptors, retinoic acid receptors (RARs) and retinoid X receptors, subsequently binding to retinoic acid response elements [9]. The latter leads to conformational changes of the DNA sequence, with the regulation of specific target genes. Of note, among the three RARs, RAR-β is known as a favorable prognostic factor in neuroblastoma patients [10].

Polyinosinic-polycytidylic acid [poly (I:C)], the synthetic agonist of Toll-like receptor 3 (TLR3), has been used as a cancer vaccine adjuvant for several types of cancer, including prostate cancer, lymphoma, lung cancer, melanoma, and hepatocellular carcinoma [11, 12]. Our previous studies have demonstrated that poly (I:C) can suppress neuroblastoma cells through accumulation of mitochondrial reactive oxygen species (ROS), and activation of apoptosis via TLR3 signaling pathways [13–15].

The combination of RA with poly (I:C) has been shown to improve treatment efficacy in prostate and breast cancer patients [16, 17]. Specifically, RA/poly (I:C) combinations can cause type I interferon (IFN)-dependent apoptosis followed by activation of caspase 8 and caspase 3, as well as induction of tumor necrosis factor-related apoptosis signaling. Enhancement of the expression of cytosolic dsRNA sensors, including melanoma differentiation-associated protein 5 (MDA-5) and retinoic acid-inducible gene I (RIG-I), demonstrates a role for RA in promoting poly (I:C)-induced innate immune responses [17].

In the present study, we treated neuroblastoma cells with different *MYCN* status with 13cRA. The *MYCN*-amplified neuroblastoma cells exhibited susceptibility to 13cRA, while *MYCN*-nonamplified neuroblastoma cells did not. Our results indicate that the combination of 13cRA and poly (I:C) effectively enhances the immunogenic response and cytotoxicity effect in 13cRA-sensitive neuroblastoma cells and endothelial cells, both in vitro and in vivo.

Materials and methods

Cell lines and cell culture

Four human neuroblastoma cell lines (SK-N-AS (CRL-2137), SK-N-FI (CRL-2142), SK-N-DZ (CRL-2149), and BE(2)-M17 (CRL-2267)) were purchased from the American Type Culture Collection (Manassas, VA, USA). Mouse endothelial cell line SVEC4–10 was obtained from the Bioresource Collection and Research Center of the Food Industry Research and Development Institute.

SK-N-AS, SK-N-FI, and SK-N-DZ cells were maintained in Dulbecco's Modified Eagle's medium supplemented with 2 mM L-glutamine. BE(2)-M17 cells were maintained in Minimum Essential Media/F-12 (1:1) medium adjusted to contain 1 mM sodium pyruvate. All culture media were supplemented with 10% (v/v) heat-inactivated fetal bovine serum, antibiotic-antimycotic solution, and10 mM nonessential amino acids. Cell cultures were maintained under 5% CO_2 atmosphere at 37 °C. The formation of neurite outgrowth and extensions of neuronal cells after treatments were examined using phase-contrast microscopy (Leica DMI 3000B, Wetzlar, Germany).

Treatment of human neuroblastoma cells with poly (I:C) and 13cRA

High molecular weight poly (I:C) (average size of 1.5–8 kb) was purchased from Invitrogen (Carlsbad, CA, USA), and 13cRA from Sigma (St. Louis, Mo, USA). To determine the effectiveness of combinational poly (I:C) and 13cRA therapy, neuroblastoma cells were administrated with 50 μg/ml poly (I:C) and/or 13cRA in different concentrations (0, 25, 50, 75, and 100 μM) for indicated times. The order of administration of 13cRA and poly (I:C) to neuroblastoma cells was performed several times to determine the best sequence to maximize treatment effectiveness. Cells were incubated with 50 μM 13cRA for the first 24 h, and then 50 μg/ml poly (I:C) for an additional 24 h sequentially, or with 50 μM 13cRA and 50 μg/ml poly (I:C) concurrently for 48 h.

Cell proliferation assay

For the cell proliferation assay, cells were plated onto each well of a 96-well plate at a density of 1×10^4–3×10^4 cells/well and cultured overnight. After treatment, cell proliferation reagent WST-1 (Roche Applied Science, Mannheim, Germany) was added, which was performed according to the manufacturer's instructions. The absorbance of the samples at 450 nm and the reference wavelength of 630 nm were measured using a 96-well spectrophotometric plate reader (Hidex Sense, Turku, Finland).

Western blot analysis

Total proteins of cells with indicated treatments were extracted by PRO-PREP™ Protein Extraction Solution (iNtRON Biotechnology; Seoul, Korea). Protein concentrations were measured using the bicinchoninic acid

assay (Bio-Rad; Richmond, CA). Thirty micrograms of total cellular proteins was separated by 10–15% sodium dodecyl sulfate polyacrylamide electrophoresis gel, and then transferred into nitrocellulose membranes.

The following primary antibodies were used: TLR3 (Abcam Inc., Cambridge, MA, USA), MDA-5 (D74E4; Cell Signaling Technology, Danvers, MA, USA), RIG-I (D14G6; Cell Signaling Technology), mitochondrial antiviral-signaling protein (MAVS, Santa Cruz Biotechnology), phosphorylated interferon regulatory factor 3 (pIRF3, pS386; BIOSS), cleaved poly ADP ribose polymerase (PARP, D214, Cell Signaling Technology), cleaved-caspase 9 (Asp330, Cell Signaling Technology), cytochrome C (Cell Signaling Technology), GAP43 (Abcam Inc.), RAR-β (Abcam Inc.), and β-actin (Millipole, Billerica, MA, USA). Goat anti-mouse and anti-rabbit secondary antibodies conjugated to horseradish peroxidase were purchased from Cell Signaling and Santa Cruz Biotechnology, respectively. Protein-antibody complexes were developed using the enhanced chemiluminescence detection kit (Amersham Pharmacia Biotech, Uppsala, Sweden), and visualized on X-ray films. Band density was measured and quantified with ImageJ (National Institutes of Health) and normalized to β-actin.

Immunofluorescence staining

For immunofluorescence staining, cells were seeded into a 6-well plate at 1×10^5 cells/well. After treatments, cells were washed with PBS, fixed in 3.7% paraformaldehyde for 10 min, and then permeabilized with 0.5% Triton X-100/PBS for 10 min at room temperature. The cells were blocked with 1% bovine serum albumin for 30 min at room temperature. After being washed with PBS, cells were labeled with F-actin staining (green, Invitrogen). Slides were co-stained with DAPI (4′,6-diamidino-2-phenylindole; Molecular Probes) to visualize the nuclei, mounted with fluorescent mounting medium (Dako Cytomation), and visualized using Olympus FluoView® confocal microscopy.

Human neuroblastoma xenograft animal model

Four-week-old male nonobese diabetic/SCID (NOD/SCID, NOD.CB17-Prkdcscid/NcrCrl) mice were purchased from the Ministry of Science and Technology, Taiwan. Proper care and procedures were approved of by the Animal Ethics Committee of the Kaohsiung Chang Gung Memorial Hospital. After 1 week of adaptation to the environment, the mice received a subcutaneous injection of 1×10^7 SK-N-DZ cells into the right flank. The tumor was induced and allowed to grow until day 8. A total of 42 mice were randomly separated into five groups. The mice then received intraperitoneal injections of the indicated treatment twice weekly for 4 weeks. Treatment groups were divided into four different treatment strategies: poly (I:C) only ($n = 8$); 13cRA only ($n = 8$); 13cRA followed by poly (I:C) sequentially ($n = 9$); and 13cRA/poly (I:C) concurrently ($n = 9$). In the control group ($n = 8$), 100 ml of normal saline or cone oil was injected as scheduled. In the treatment groups, poly (I:C) (10 mg/kg dissolved in normal saline) and/or 13cRA (5 mg/kg dissolved in cone oil) was injected in accordance with the courses described in the Supplemental Data. Caliper measurement of tumor size was documented every 3 days. Mice were anesthetized using an intraperitoneal injection of 40 mg/kg Zoletil plus 5 mg/kg Xylazine. Euthanasia was humanely conducted when animals presented reduction of body weight over 25% or tumor diameter > 2 cm^3.

Immunohistochemistry

Paraffin-embedded tissue sections (5 mm thick) of xenograft tumors were deparaffinized and rehydrated. Endogenous peroxidase activity was inactivated with 3% hydrogen peroxide for 15 min, followed by processing in the microwave oven with 10 mM citrate buffer (pH 6.0) to unmask epitopes. After antigen retrieval, the sections were incubated with diluted primary antibodies isolectin IB4-biotin conjugates (Molecular Probes, 1:200, 30 min) or α-thalassemia/mental retardation syndrome X-linked (ATRX) (Genetex, 1:200, 2 h), and then detected by a streptavidin horseradish peroxidase product (BD Pharmingen) for 30 min, and finally developed with DAB. After extensive washing, the sections were incubated for 3 min with peroxidase substrate diaminobenzidine, counterstained with Gill's hematoxylin, and mounted in mounting medium.

Quantification of staining density

For ATRX staining, we randomly selected five high-power (×400) fields for each section to evaluate each sample. The intensity of positive staining tumor cells was scored as 0 = none; 1 = weak; 2 = intermediate; and 3 = strong. The proportion of each intensity score was further scored as: 0 = no positive cells; 1 = 0–20%; 2 = 21–50%; 3 = 51–80%; 4 = 81–100%. Both scores were multiplied and summed to produce a final immunoreactivity score, ranging from 0 to 12.

To quantify the endothelial cell density in the xenografted tumor, the vascular areas (hot spots) with the highest density of endothelial cells were chosen and photographed for analysis using ImageJ. Five images (×200 magnification) were selected in each tumor section with care to avoid areas of necrosis. Color-discrimination thresholds were determined in the positively stained areas with a minimum threshold of 500 pixels. The endothelial cell density was calculated as the average of the isolectin IB4-positively

stained regions of each tumor section (positively stained area pixels/total pixels).

Measurement of cell apoptosis and death

Cell apoptosis was quantitatively assessed by double-staining with fluorescein isothiocyanate (FITC)-conjugated Annexin V and propidium iodide (PI) using the Annexin V FITC Apoptosis Detection kit (BD Biosciences). The stained cells were evaluated in the fluorescence-activated cell sorting Calibur and analyzed using CellQuest software (BD Biosciences). Four cellular subpopulations evaluated: viable cells (Annexin V^-/PI^-); early apoptotic cells (Annexin V^+/PI^-); late apoptotic cells (Annexin V^+/PI^+); and necrotic/damaged cells (Annexin V^-/PI^+). Annexin V^+ cells were considered to be apoptotic cells. Caspase 3 activity were measured by the caspase 3 assay kit according to the manufacturer's instructions (Abcam).

TUNEL assay for paraffin-embedded tissue sections

TUNEL staining was performed on paraffin-embedded tissue sections of xenograft tumors to assess cellular apoptosis by using the In Situ Cell Death Kit (Cat.No.12156792 910; Sigma-Aldrich, Germany). Five-micrometer sections were deparaffinized, treated with 3% hydrogen peroxide to inactivate the endogenous peroxidase activity, and microwaved for 7 min in 10 mM citrate buffer (pH 6.0) to retrieve the antigen. The sections were then incubated in PBS supplemented with 5% fetal calf serum for 10 min to block background interactions. The sections were then incubated with TUNEL reaction mixture for 45 min at 37 °C in a humidified atmosphere in the dark. The sections were co-stained with DAPI to visualize the nuclei. The stained sections were mounted with fluorescent mounting medium (Dako Cytomation) and examined by a fluorescence microscope (Leica DMI 3000B, Wetzlar, Germany).

Statistical analysis

Results were analyzed using two-tailed Student's *t* tests. Data shown are representative of at least three independent experiments. Data were expressed as the mean ± standard deviation or mean ± standard error of the mean. $P < 0.05$ was regarded as statistically significant.

Results

13cRA has an inhibitory effect on proliferation of *MYCN*-amplified neuroblastoma cell lines

To evaluate the sensitivity of 13cRA in different neuroblastoma cells, we investigated two *MYCN*-nonamplified (SK-N-AS and SK-N-FI) and another two *MYCN*-amplified (SK-N-DZ and BE(2)-M17) cell lines. A number of viable cells were calculated at the indicated time points after exposure to different doses of 13cRA (0, 50, 75, and 100 μM) for 24 or 48 h. As shown in Fig. 1, a marked dose-dependent decrease in cell survival rate was observed in both *MYCN*-amplified neuroblastoma cells, which reached significance in SK-N-DZ cells upon incubation with 13cRA ($P < 0.05$). 13cRA treatment has little effects on the growth of both *MYCN*-nonamplified cells. We have treated 13cRA-sensitive SK-N-DZ cells with lower concentration (1–100 μM) and more extended periods (1–7 days) and measured the cell proliferation using the WST-1 assay. The result has been shown in Supplementary Fig. S1. The lower concentration of 13cRA (below 25 μM) took a longer time (more than 4 days) to achieve IC50. The higher concentration of 13cRA (above 50 μM) took only 2 days to reach IC50.

In the clinical practice, only limited clinical benefits had been observed in patients receiving low-dose 13cRA (0.75 mg/kg/day). The higher dose intermittent schedule of 13cRA (160 mg/m^2/day in two divided doses for 14 days

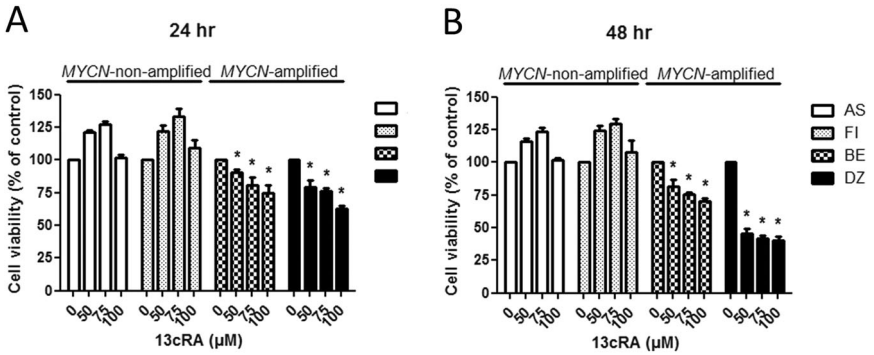

Fig. 1 The treatment effect of 13cRA on neuroblastoma cell lines. Neuroblastoma cells were treated with varying concentrations of 13cRA for 24 h (**a**) or 48 h (**b**). The cell viability was measured by the WST-1 assay. The results are shown as a percentage of the values obtained in control conditions. All values are shown as the mean ± S. D. of three different experiments. AS: SK-N-AS cells, FI: SK-N-FI cells, BE: BE(2)-M17 cells, DZ: SK-N-DZ cells.(*$P < 0.05$ compared with control group).

every 28 days) prescribed after intensive therapy resulted in significant improvement in 5-year overall survival rates on the high-risk neuroblastoma patients [6]. To mimic clinical pulsed high-dose treatment schedule and avoid adverse side effects after long-term exposure [18–21], we selected the effective high concentration of 13cRA at 50 μM for subsequent experiments.

Sequential 13cRA followed by poly (I:C) enhances the inhibitory effect on 13cRA-sensitive neuroblastoma cells

In our previous study, in contrast to *MYCN*-nonamplified SK-N-AS cells, poly (I:C) had limited inhibitory effects on proliferation of *MYCN*-amplified SK-N-DZ cells [15]. Recently, Bernardo et al. reported that the combination of RA and poly (I:C) promotes the apoptotic response in breast cancer cells by induction of dsRNA receptors and downstream apoptotic signaling [17]. We therefore decided to investigate the effects of the combination of 13cRA and poly (I:C) in SK-N-DZ cells, treated sequentially or concurrently. The treatment protocol is described in detail in Supplementary Fig. S2A.

The results demonstrated that single-agent treatment with 13cRA significantly suppressed the growth of SK-N-DZ cells with dose-dependent and time-dependent manner, and the inhibition effect was prominent with treatment for 48 h (Fig. 2a). Of note, the additional 24 h of 50 μg/ml poly (I:C) after 13cRA induced an enhanced inhibitory effect on cell growth. In contrast, the enhanced inhibitory effect was not observed in the concurrent treatment of 13cRA and poly (I:C) for 48 h (Fig. 2a). We calculated the IC50 value of 13cRA treatment with or without poly (I:C) under the treated period of 48 h. Treatment of 13cRA or 13cRA with poly (I:C) concurrently for 48 h could achieve growth inhibition >50%, and the value of IC50 was 38.92 and 37.92 μM, respectively. However, treatment of 13cRA for only 24 h or sequential 13cRA 24 h followed by poly (I:C) 24 h was unable to achieve IC50 in such experimental condition.

Immunogenic response and apoptotic pathway were involved in 13cRA/poly (I:C) combination therapy in neuroblastoma cells

To clarify the mechanism at play in the 13cRA/poly (I:C) treatment, we determined the 13cRA-induced apoptotic response by the Annexin V-PI assay with flow cytometry in vitro (Fig. 2b). Compared with control and poly (I:C) only, 13cRA-contained-treatment induced significantly higher apoptotic rate in SK-N-DZ cells. Pretreatment of SK-N-DZ cells with 13cRA for 24 h, followed by further poly (I:C) treatment resulted in a significant increased apoptotic rate than the single agent with poly (I:C) or 13cRA alone. Next, we analyzed the expression of dsRNA-related and apoptosis-associated markers (Fig. 2c, d). In SK-N-DZ cells, poly (I:C) treatment alone was unable to induce expression of dsRNA-related proteins. In contrast, single-agent treatment with 13cRA-induced visible expression of TLR3, MAVS, and IRF3 in time-dependent manners. Furthermore, both sequential and concurrent treatments of 13cRA and poly (I:C) enhanced the synergistic effect on the induction of innate immunogenic-related proteins, including TLR3, MAVS, and pIRF3, but not MDA-5 or RIG-I (Fig. 2c).

In addition, the combined 13cRA/poly (I:C) treatment more effectively reinforced expression of apoptosis-related proteins, including cleaved-PARP, cleaved-caspase 9, and cytochrome C, compared with single-agent treatment (Fig. 2d). Due to barely detected expression of caspase 3 by western blot, we measured the caspase 3 activity of SK-N-DZ cells (Supplementary Fig. S2B). In our previous study, poly I:C treatment activated caspase 3 expression in SK-N-AS cells [13]. So, high detectable caspase 3 activity of SK-N-AS cell was used as the positive control. However, the caspase 3 activity is much lower in SK-N-DZ cells and is unequal to the ratio of Annexin V-PI staining. So, caspase 3 may be not a suitable marker of apoptotic response in SK-N-DZ cells.

Taken together, the results demonstrated that 13cRA/poly (I:C) combination therapy in SK-N-DZ neuroblastoma cells could enhance cellular immunogenic response and promote apoptotic signaling, when treated either sequentially or concurrently.

13cRA-contained treatment inhibits tumor growth in neuroblastoma xenografted mice

We investigated the combined therapeutic effect of 13cRA/poly (I:C) using a human neuroblastoma xenograft model. Eight days after injection, we randomly separated the mice into five groups. All groups were treated as described in Supplementary Fig. S3A. The initial tumor volume of the five groups showed no difference before treatment Supplementary Fig. S3B. After treatment for 4 weeks, we observed a significant decrease in the tumor growth rate of the 13cRA-contained therapy, including 13cRA alone, concurrent, and sequential 13cRA and poly (I:C) treatment groups, compared with the control and poly (I:C) alone groups $P < 0.05$, Supplementary Fig. S3C). The lowest tumor growth rate was observed in the concurrent 13cRA and poly (I:C) group (Group 5) compared with the other groups. Although poly (I:C) treatment inhibited tumor development, the 13cRA-contained treatment significantly suppressed the tumor volume and tumor weight, compared with the control and poly (I:C) groups (Fig. 3a, b). To further clarify whether cell apoptosis contributes to suppressing tumor growth, we also performed TUNEL staining

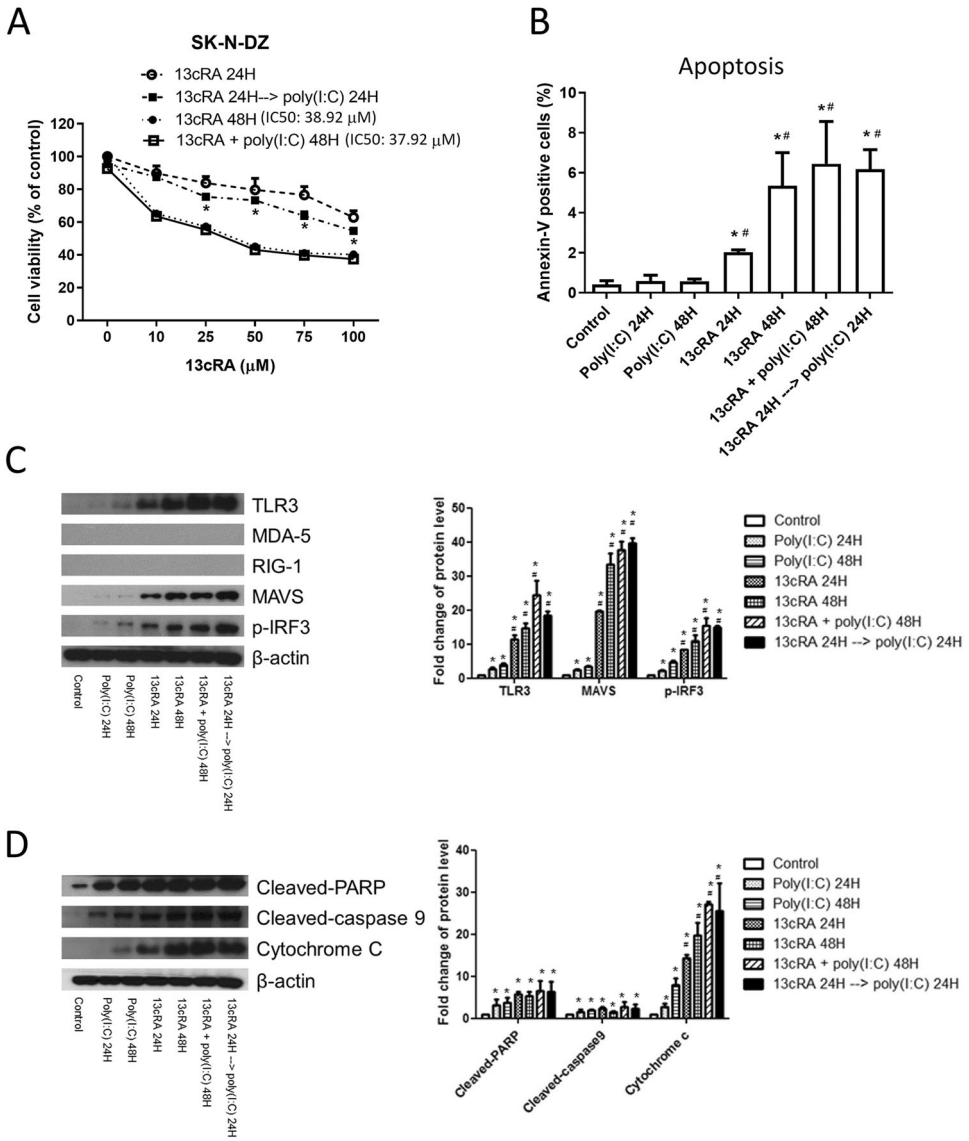

Fig. 2 Combined treatment of 13cRA with poly (I:C) enhances the growth inhibition and immunogenic apoptosis response in 13cRA-sensitive cells. a Cells were treated with varying concentrations of 13cRA in the presence or absence of poly (I:C) (50 μg/ml) for 48 h. Cell proliferation was then measured by the WST-1 assay. The results are shown as a percentage of the values obtained in control condition. IC50 was calculated using software Prism 7.0. All values are shown as the mean ± S.D. of three different experiments. (Asterisks denote statistically significant differences between 13cRA for 24 h followed by poly (I:C) for 24 h compared with equal dose of 13cRA for 24 h). **b** Cell death was assayed by Annexin-PI staining and flow cytometry analysis in SK-N-DZ cells after treatment with poly (I:C), 13cRA or combination therapy. Annexin V-positive cells were recognized as apoptotic cells. ($^{*}P < 0.05$ compared with control group; $^{\#}P < 0.05$ compared with poly (I:C) for 24 h). **c** Immunoblot demonstrated the protein levels of TLR3, MDA-5, RIG-1, MAVS, and phosphorylated IRF3 (pIRF3) after treatment with 13cRA (50 μM) and poly (I:C) (50 μg/ml) either sequentially or concurrently for 48 h. β-Actin was used as loading control. The immunoblots showed representative results from three independent experiments. The expression of MDA-5 and RIG-1 was barely detected in SK-N-DZ cells. The expression ratio of other proteins was quantified by densitometer determination and normalized relative to β-actin. ($^{*}P < 0.05$ compared with control group; $^{\#}P < 0.05$ compared with poly (I:C) for 24 h). **d** Immunoblot showed the expression levels of cleaved-PARP, cleaved-caspase 9, and cytochrome C after treatment with 13cRA (50 μM) and poly (I:C) (50 μg/ml) either sequentially or concurrently for 48 h. β-Actin was used as loading control. The immunoblots showed representative results from three independent experiments. The expression ratio was quantified by densitometer determination and normalized relative to β-actin.($^{*}P < 0.05$ compared with control group; $^{\#}P < 0.05$ compared with poly (I:C) for 24 h).

in xenografted tumor tissue. The tumor tissues exhibited significantly more TUNEL-positive staining in 13cRA-contained treatment groups, but not in the control and poly (I:C) groups (Supplementary Fig. S4). These results suggest that 13cRA-contained therapy acts to suppresses tumor growth in vivo through inducing tumor cell apoptosis.

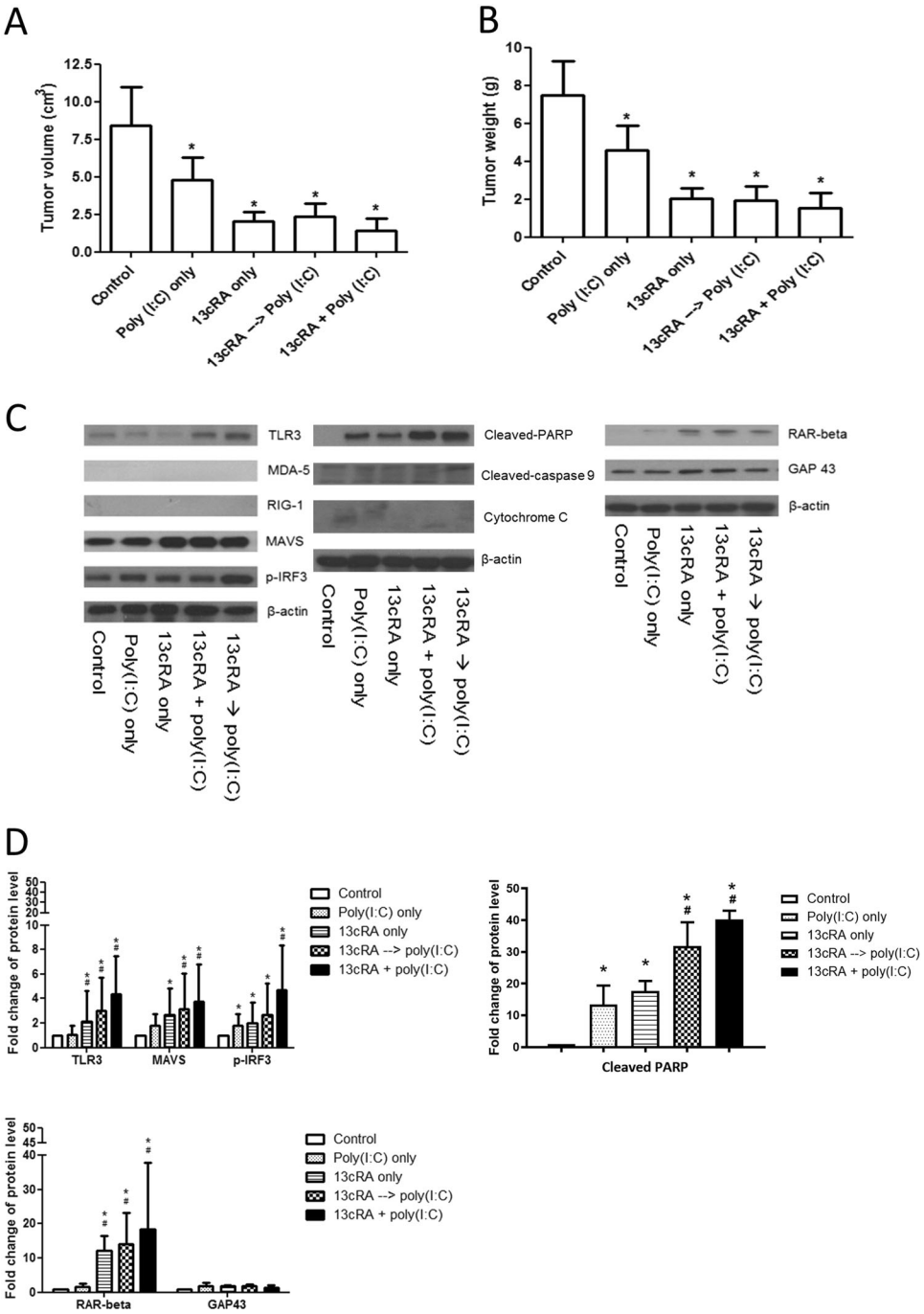

Fig. 3 The treatment effect of 13cRA and poly (I:C) on xenograft mice. SK-N-DZ cells (1×10^7 cells) was injected subcutaneously into the right flank of male NOD/SCID mice. Treatment groups were randomly dived into five different strategies: control, poly (I:C) only, 13cRA only, 13cRA followed by poly (I:C) sequentially and 13cRA with poly (I:C) concurrently. Tumor size (**a**) and tumor weight (**b**) of xenografted tumors on the day of sacrifice in different groups were measured. Data are expressed as means ± SEM. (*$P < 0.05$ compared with the control group). **c** Western blot analysis revealed the expression of protein levels of immunogenic response (TLR3, MDA-5, RIG-1, MAVS, and pIRF3), apoptotic response (cleaved-PARP, cleaved-caspase 9, and cytochrome C), and neural differentiated markers (RAR-β and GAP43) in the xenografted tumors. Additional poly (I:C) injection either sequentially or concurrently enhanced the effect of a single agent with 13cRA or poly (I:C). β-Actin was used as loading control. The immunoblots show representative results from three independent experiments. **d** The expression of MDA-5, RIG-1, cleaved-caspase 9, and cytochrome C was barely detected in tumor tissue. The expression ratio of other proteins was quantified by densitometer determination and normalized relative to β-actin. (*$P < 0.05$ compared with control group; #$P < 0.05$ compared with poly (I:C) only).

13cRA/poly (I:C) enhances the expression of immunogenic response and apoptotic pathway in neuroblastoma xenografted mice

To assess the in vivo effects of 13cRA and poly (I:C) in neuroblastoma xenografts, western blotting of the tissue homogenates was performed (Fig. 3c, d). Significant increases of TLR3, pIRF3, and MAVS were found both in the sequential 13cRA followed by poly (I:C) group, and the concurrent 13cRA with poly (I:C) group. In addition, apoptotic protein cleaved-PARP was notably induced in the 13cRA/poly (I:C) treatment groups. Furthermore, 13cRA-contained therapy also upregulated the expression of RAR-β, the major mediator required for the antiproliferative effects exerted by retinoids in tumor tissues [22]. These results corroborated the findings of the in vitro model.

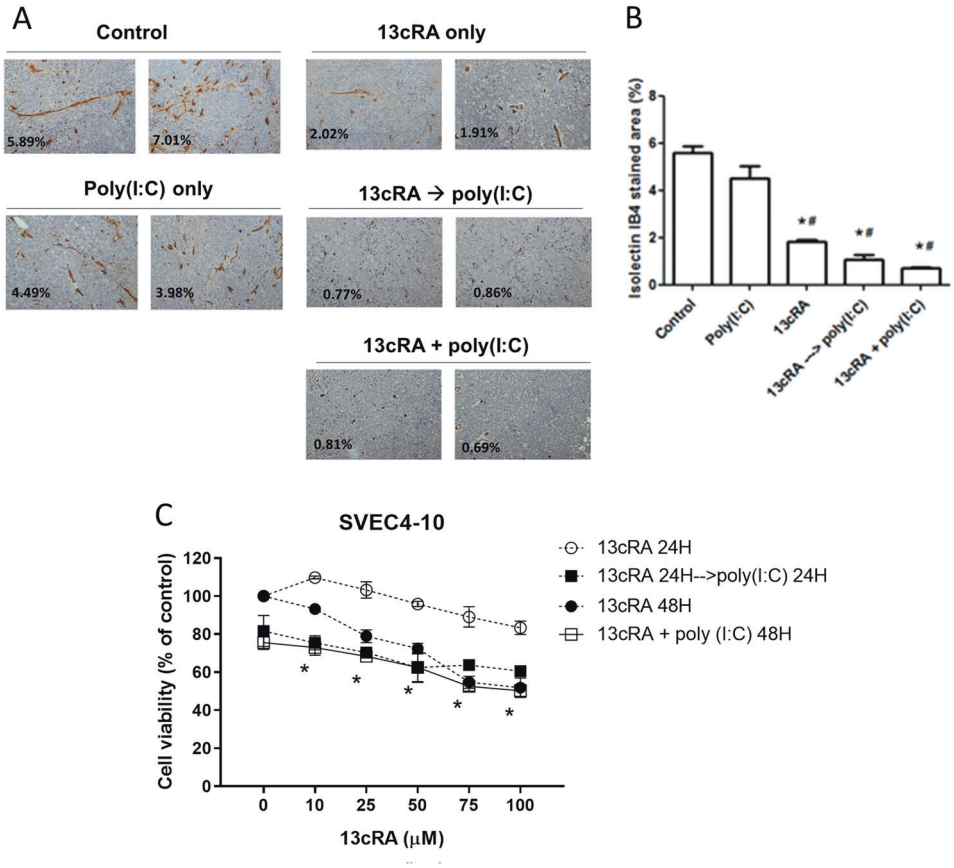

Fig. 4 Poly I:C enhances the 13cRA-induced inhibitory effect of angiogenesis. a The tissue section of DZ xenografts tumor was stained with isolectin IB4. The representative images of xenografted tumors collected at the end of the experiments of different groups are presented (original magnification, ×200). The quantification value of positive isolectin IB4 area is labeled on each representative image. **b** Five different microscopic fields were taken per sample. Data are expressed as mean ± SD (*$P < 0.05$ compared with control group, $^{\#}P < 0.05$ compared with poly (I:C) only group). **c** The mouse endothelial cell line SVEC4–10 cells were treated with varying concentrations of 13cRA in the presence or absence of poly (I:C) (50 μg/ml) for 48 h. The cell viability was measured by the WST-1 assay. In SVEC4–10 cells, added poly (I:C) enhanced the growth inhibitory effect compared with 13cRA only. The results are shown as a percentage of the values obtained in control conditions. All values are shown as the mean ± S. D. of three different experiments. (*$P < 0.05$ compared with 13cRA for 24 h).

13cRA/poly (I:C) inhibits the growth of endothelial cells both in vivo and in vitro

In contrast to the in vitro observations, 13cRA with or without poly (I:C) could effectively suppress tumor growth in the xenograft model. We hypothesized that 13cRA may not only affect the growth of the tumor cell but may also affect the tumor microenvironment. We therefore assessed the vessel formation and vascular density of tumor specimens using the immunohistochemistry of isolectin IB4 (Fig. 4a), which labels the endothelial cells explicitly. A significant reduction in the number of tumor vessels was shown in DZ xenografts in the treatment groups containing 13cRA (Fig. 4b). To confirm the direct effect of 13cRA in the inhibition of angiogenesis, the mouse endothelial cell line SVEC4–10 cells were treated with 13cRA and poly I:C concurrently for 48 h. As shown in Fig. 4c, poly I:C significantly enhanced the inhibitory effect of 13cRA in SVEC4–10 cells.

As shown in Fig. 5a–c, treatment of SVEC cells with 13cRA and poly (I:C) up to 48 h resulted in less protruding filopodia formation on the cell surface and a notable decrease of intracellular F-actin, compared with the poly (I:C) or 13cRA alone groups. The results indicated that the combination of 13cRA and poly (I:C) inhibits the formation of filopodia and derangement of F-actin, leading to the observed reduction of tumor vessel formation in the xenograft model.

Compared with poly (I:C), 13cRA alone induced notable expression of TLR3, pIRF3, MAVS, cleaved-PARP, cleaved-caspase 3 and 9, and cytochrome C in a dose-dependent manner in SVEC4–10 cells (Fig. 6a). When combined with 13cRA, poly (I:C) synergistically enhanced the apoptotic effect of 13cRA (Fig. 6b).

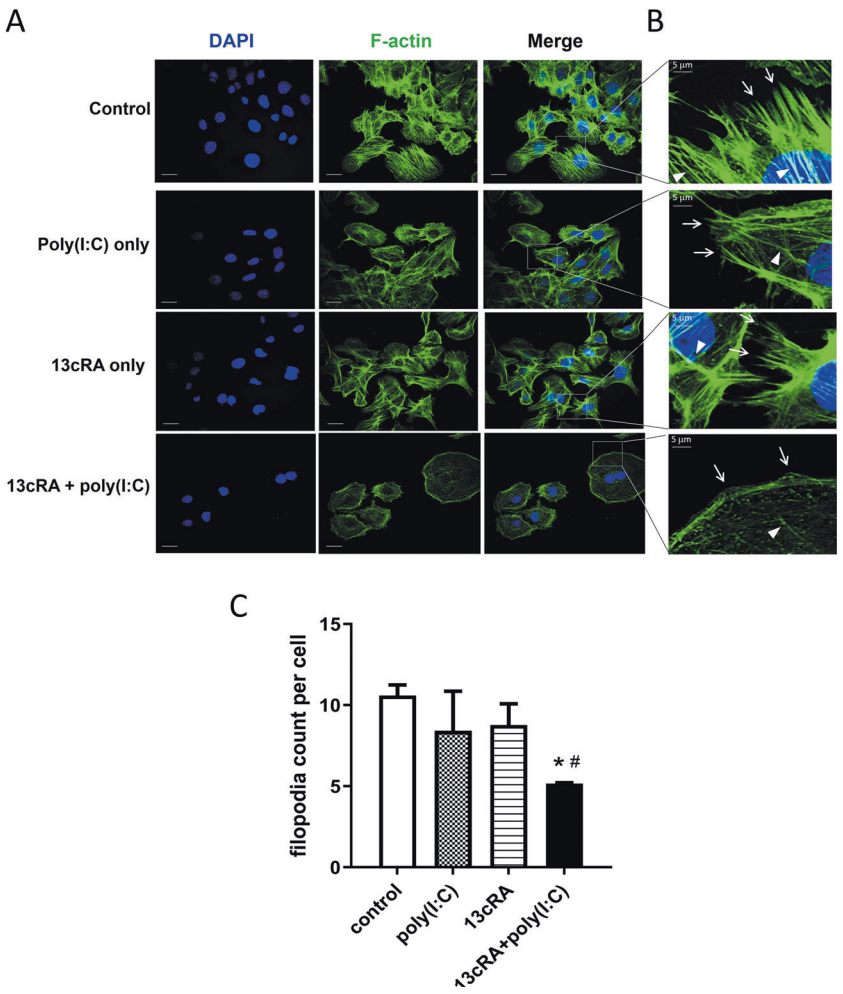

Fig. 5 13cRA affects the cytoskeleton structure of endothelial cells. a After 48 h of 13cRA or poly (I:C) treatment, SVEC4–10 cells were stained by anti-F-actin (green) and DAPI (blue). Cells were visualized by a confocal microscopy. Scale bar, 20 μm. **b** In the higher magnification view, white arrowhead and arrow indicate F-actin bundle, and filopodia, respectively. Control cells present organized F-actin bundle and distinct formation of filopodia. In contrast, cells treated with combined 13cRA and poly (I:C) have disorganized F-actin bundle and impaired formation of filopodia. Experiments were performed in triplicate, and three fields from each well were imaged. Scale bar, 5 μm. **c** The number of filopodia was counted from a 200 x 250 μm image field with most abundant cells from at least three images of independent experiments for each group. Data are presented as mean ± SD (*$P < 0.05$ compared with control group, #$P < 0.05$ compared with poly (I:C) only group).

The combination of 13cRA and poly (I:C) induces redifferentiation in neuroblastoma cells

We further analyzed the expression of RAR-β and GAP43, a common marker of differentiating neurons, in neuroblastoma cell lines after treatments. As shown in Fig. 7a, b, RAR-β and GAP43 expression was significantly increased after 13cRA/poly (I:C) treatment in SK-N-DZ cells. We also investigated the morphologic characteristic of neuroblastoma cells after 13cRA/poly (I:C) treatment. Although poly (I:C) induced few neurite growths, 13cRA-contained treatment induced more extended neurite-like structures, and branching of the outgrowths in SK-N-DZ cells (Fig. 7c). Because of the low adhesion property of SK-N-DZ cells, it is difficult to prevent the detachment and loss of cells during the process of immunofluorescent staining. We determined neural differentiation maker by targeting GAP43 level using flow cytometry alternatively. The result demonstrated that 13cRA-contained treatment induced significantly higher expression of GAP43 in SK-N-DZ cells, no matter with or without poly (I:C) (Supplementary Fig. S5).

The *ATRX* gene mutation was detected in 44% of neuroblastoma patients older than 12 years, often associated with a poor prognosis [23]. The inactivating *ATRX* mutation is associated with an absence of the ATRX protein in the nucleus. Immunohistochemistry confirmed ATRX protein expression in xenograft tumors. After 13cRA-contained treatment, the nuclear expression of ATRX was significantly induced in the tumor tissue, particularly in the concurrent 13cRA/poly (I:C) group (Fig. 8). These results indicated that the combination of poly (I:C) and 13cRA induces differentiation protein ATRX in neuroblastoma cells, leading to tumor reduction with favorable tumor behavior.

Discussion

In the present study, we demonstrate that poly (I:C) could enhance the antitumor effect of 13cRA in *MYCN*-amplified neuroblastoma cells. The combination of 13cRA and poly (I:C) synergistically induces the expression of TLR3 and MAVS, thus amplifying the apoptotic response through the

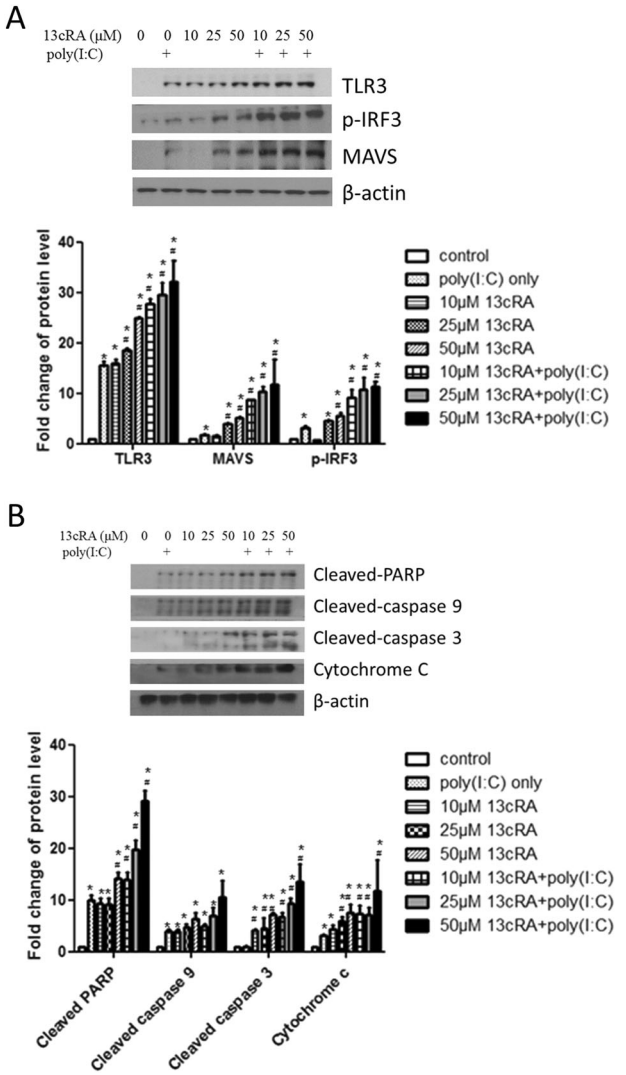

Fig. 6 Poly I:C enhances the 13cRA-induced immunogenic apoptosis response in endothelial cells. Western blot analysis revealed the expression of protein levels of (**a**) immunogenic response (TLR3, MAVS, and pIRF3) and (**b**) apoptotic response (cleaved-PARP, cleaved-caspase 9, cleaved-caspase 3, and cytochrome C) of SVEC4–10 endothelial cells treated with 13cRA (10, 25, and 50 μM) and poly (I:C) (50 μg/ml) either alone or combination for 48 h. 13cRA and poly (I:C) cooperated to induce the remarkable expression of immunogenic-related and apoptotic-related proteins in SVEC4–10 cells. β-Actin was used as loading control. The immunoblots show representative results from three independent experiments. The expression ratio was quantified by densitometer determination and normalized relative to β-actin. (*$P < 0.05$ compared with control group; $^{\#}P < 0.05$ compared with poly (I:C) alone).

mitochondrial signaling pathway. Our findings further suggest that combined treatment with poly (I:C) could enhance the immunogenic and apoptotic effects in those 13cRA-responsive cancer cells and endothelial cells both in vitro and in vivo. Thus, innate immune modulators may exert synergistic benefits in high-risk neuroblastoma patients with 13cRA therapy.

Retinoids are frequently combined with other chemotherapies to treat a variety of cancers, such as tamoxifen, paclitaxel, and IFN for treatment of breast cancer, or paclitaxel, and cisplatin for treatment of advanced non-small cell lung cancer [24, 25]. In high-risk neuroblastoma, 13cRA is also used in combination with immunotherapeutic agents, such as aldesleukin, leukine, or unituxin [26]. The activated RA pathway may induce neuroblastoma cell differentiation, neuroblastoma cell senescence via the PI3K/AKT pathway, downregulate *MYCN* expression, suppress hypoxia-inducible factors activation, and regulate redox balance [27–31]. However, patients undergoing RA therapy often suffer from side effects when administered higher doses or over extended treatment periods [19–21].

It has been demonstrated that 13cRA can regulate immunomodulatory TNF-related apoptosis-inducing ligand signaling and type I IFN through cotreatment with poly (I:C) in breast cancer cells [17, 32, 33]. In a recent clinical trial of patients with recurrent or metastatic head and neck squamous cell cancer and melanoma, intratumoral injection of the synthetic dsRNA complex was well-tolerated by patients, and induced local/systemic immune response [34]. These studies suggest that RA/poly (I:C) combination therapy may be an effective clinical treatment for recurrent neuroblastoma patients, particularly in the prevention of resistance to RA.

Previous in vitro studies have used long-term exposure to low-dose 13cRA (1–10 μM) to investigate the regulatory mechanism, and effectiveness of 13cRA in cell lines [35, 36]. Despite limited clinical benefits observed in patients receiving low-dose 13cRA, a high dose (160 mg m^{-2} day^{-1}) of 13cRA administration with an intermittent regimen significantly improves the 3-year event-free survival rate [37–39].

In this study, we demonstrate that preexposure to high-dose 13cRA over a short-term period could restore immunogenic signaling through inducible TLR3 expression in poly (I:C)-resistant SK-N-DZ cells. The subsequent synthetic poly (I:C) treatment leads to activation of downstream apoptotic caspase responses, and inhibition of tumor formation in a xenograft model. Notably, this combination therapy did not induce the expression of MDA-5 or RIG-I, only activating enhanced levels of TLR3, MAVS, and pIRF3 in SK-N-DZ cells. Although MAVS is the universal immunogenic adaptor of cytosolic dsRNA sensors, 13cRA-induced MAVS expression may occur through other regulatory mechanisms [40]. Thus, the interaction between 13cRA and MAVS requires further investigation.

This study further revealed that 13cRA suppressed vessel formation in a mouse xenograft model. In the 13cRA-contained treatment groups, the vascular structure and density were significantly suppressed compared with the control group. Further in vitro experiments with mouse endothelial cells confirmed the direct growth inhibitory

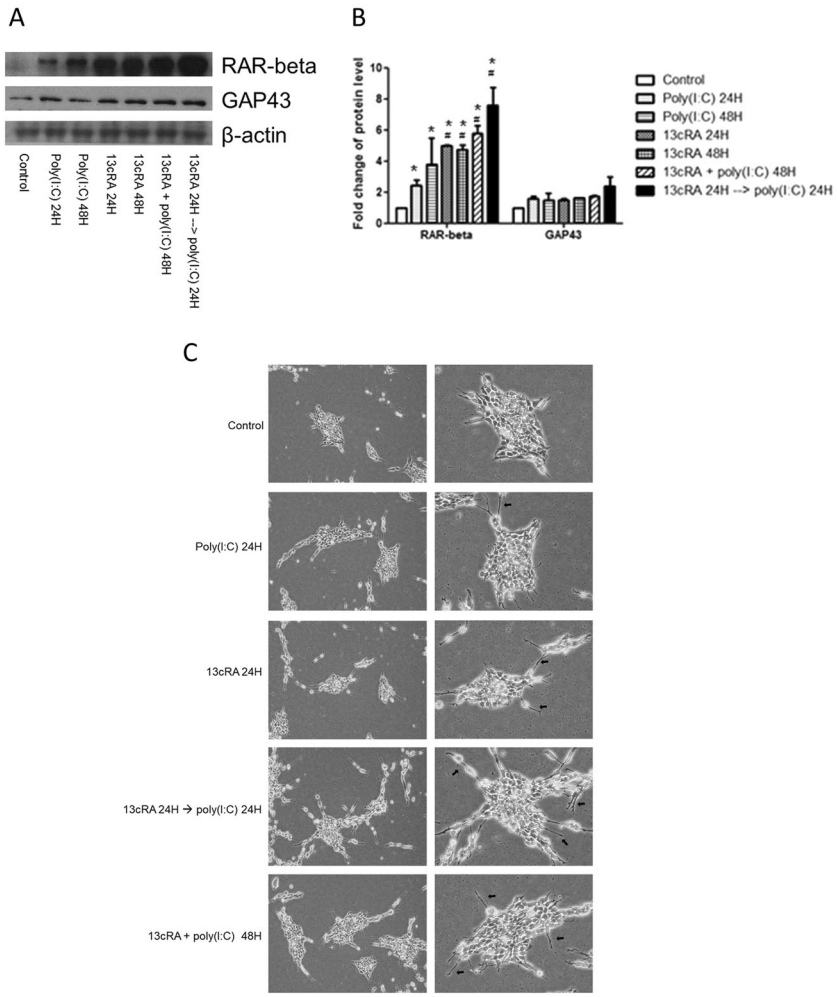

Fig. 7 13cRA induces redifferentiation of neuroblastoma cells. a Western blot analysis revealed the expression of protein levels of RAR-β and GAP43 of SK-N-DZ cells treated with 13cRA (50 μM) and poly (I:C) (50 μg/ml) either alone or combination for 48 h. 13cRA-contained treatment induced significant expression of RAR-β and GAP43. β-Actin was used as loading control. The immunoblots showed representative results from three independent experiments. **b** The expression ratio was quantified by densitometer determination and normalized relative to β-actin. (*$P < 0.05$ compared with control group; #$P < 0.05$ compared with poly (I:C) alone). **c** Cells were treated with 13cRA (50 μM) or poly (I:C) (50 μg/ml) either alone or sequentially for 24 h. The phase-contrast photomicrographs of SK-N-DZ cells after indicated treatment were displayed. 13cRA-contained treatment induced more extended neurites outgrowth. Black arrows indicated the neurite-like structures.

effect of 13cRA. Combination of 13cRA and poly (I:C) induced a similar apoptotic effect through immunogenic response with activation of TLR3 and downstream apoptotic-related proteins in endothelial cells. In addition, 13cRA/poly (I:C) combination treatment affected the cytoskeleton formation of endothelial cells by decreasing numbers of actin microfilaments and filopodia formation. Previous studies have demonstrated that the expression of RAR-β could restore RA-mediated anticancer effects by increasing the expression of migration-related proteins, such as E-cadherin, c-Src, and N-Myc, leading to rearrangement of cytoskeletal stress fibers and inhibition of cell migration [31, 41]. Our results confirm that the combination of 13cRA and poly (I:C) may suppress the growth and movement of endothelial cells through restoring the expression of RAR-β.

The precise mechanisms by which 13cRA induces differentiation are unclear. The typical characteristics of RA-induced morphologic differentiation include the formation of long neurites, cellular enlargement, and vacuolization, and formation of large, flattened fibroblastic-like cells [42]. Our study data demonstrate that the combination of 13cRA and poly (I:C) upregulated the expression of RAR-β with significant cell neurite formation, regardless of treatment sequence. In our previous studies, poly (I:C) also promoted cell differentiation through induction of endoplasmic reticulum stress to increase glucose-regulated protein 78 expression in neuroblastoma cells [13, 14]. In the present study, 13cRA/poly (I:C) combination therapy induced more apoptotic death and higher ROS production in SK-N-DZ cells (Supplementary Fig. S6). It is known that poly (I:C) could also induce the demethylation and reexpression of RAR-β via microRNAs induced by TLR3 activation in prostate and breast cancer cells [16].

In the present study, we also observed the activation of ATRX expression in tumor tissue after 13cRA treatment. ATRX plays a critical role in the maintenance of chromosome stability and regulation of lengthening of the telomeres pathway [43]. Of note, ATRX loss has been associated with higher cancer stage and poor survival outcome of patients with pancreatic neuroendocrine tumors [44]. Reactivation of nuclear ATRX in tumor cells may promote chromosome stability to inhibit tumor growth.

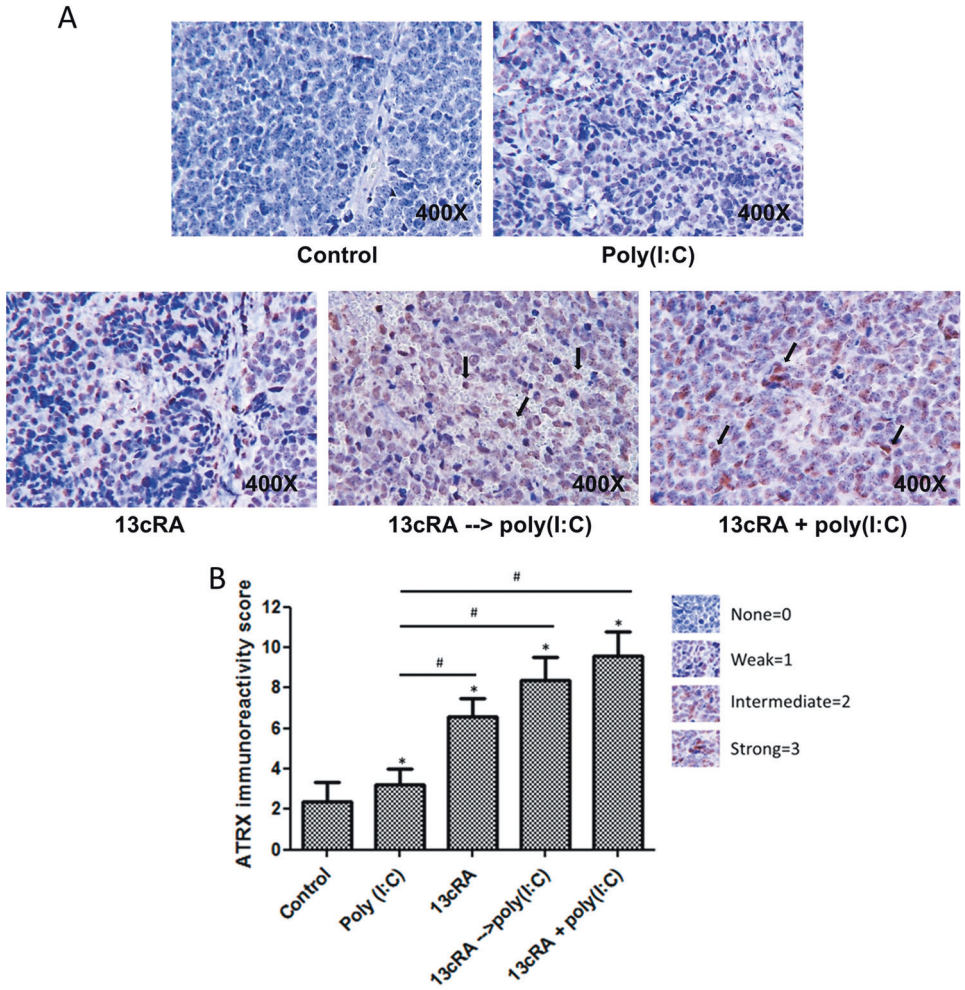

Fig. 8 Immunostaining of ATRX in xenografted tumors. **a** Strong nuclear staining of ATRX in cancer cells (black arrows) was detected in the tumors treated with 13cRA-contained treatments (original magnification, ×400). **b** The ATRX staining intensity was evaluated using immunoreactivity score ranged from 0 to 12. The 13cRA-contained groups demonstrated the significant higher ATRX score compared with control and poly (I:C) groups. (*$P < 0.05$ compared with control group, #$P < 0.05$ compared with poly (I:C) alone).

This study demonstrates that 13cRA/poly (I:C) combination therapy is more effective than single-agent therapy through activation of RAR-β and ATRX, and promotion of neuroblastoma cell differentiation to increase treatment toxicity. Poly (I:C) can effectively synergize with 13cRA to enhance the antitumor efficacy in neuroblastoma cells through upregulation of innate immune signaling and downstream apoptotic reaction, both in neuroblastoma cells and endothelial cells. Therefore, the combination of innate immune modulators with RA may enhance therapeutic effectiveness for high-risk neuroblastoma patients.

Acknowledgements This study was supported by a grant from the Chang Gung Memorial Hospital (CMRPG8F0311-3).

Compliance with ethical standards

Conflict of interest The authors declare that they have no conflict of interest.

Publisher's note Springer Nature remains neutral with regard to jurisdictional claims in published maps and institutional affiliations.

References

1. Amoroso L, Haupt R, Garaventa A, Ponzoni M. Investigational drugs in phase II clinical trials for the treatment of neuroblastoma. Expert Opin Investig Drugs. 2017;26:1281–93.
2. Kholodenko IV, Kalinovsky DV. Neuroblastoma origin and therapeutic targets for immunotherapy. J Immunol Res. 2018; 2018:7394268.
3. Parikh NS, Howard SC, Chantada G, Israels T, Khattab M, Alcasabas P, et al. SIOP-PODC adapted risk stratification and treatment guidelines: recommendations for neuroblastoma in low- and middle-income settings. Pediatr Blood Cancer. 2015;62:1305–16.
4. Nakagawara A, Li Y, Izumi H, Muramori K, Inada H, Nishi M. Neuroblastoma. Jpn J Clin Oncol. 2018;48:214–41.
5. Dragnev KH, Petty WJ, Dmitrovsky E. Retinoid targets in cancer therapy and chemoprevention. Cancer Biol Ther. 2003;2:S150–6.
6. Matthay KK, Reynolds CP, Seeger RC, Shimada H, Adkins ES, Haas-Kogan D, et al. Long-term results for children with high-risk neuroblastoma treated on a randomized trial of myeloablative therapy followed by 13-cis-retinoic acid: a children's oncology group study. J Clin Oncol. 2009;27:1007–13.
7. Tang XH, Gudas LJ. Retinoids, retinoic acid receptors, and cancer. Annu Rev Pathol. 2011;6:345–64.
8. Hansen LA, Sigman CC, Andreola F, Ross SA, Kelloff GJ, De Luca LM. Retinoids in chemoprevention and differentiation therapy. Carcinogenesis. 2000;21:1271–9.

9. Lotan R. Retinoids in cancer chemoprevention. FASEB J. 1996;10:1031–9.
10. Cheung B, Hocker JE, Smith SA, Reichert U, Norris MD, Haber M, et al. Retinoic acid receptors beta and gamma distinguish retinoid signals for growth inhibition and neuritogenesis in human neuroblastoma cells. Biochem Biophys Res Commun. 1996;229:349–54.
11. Matsumoto M, Seya T. TLR3: interferon induction by double-stranded RNA including poly(I:C). Adv Drug Deliv Rev. 2008;60:805–12.
12. Ammi R, De Waele J, Willemen Y, Van Brussel I, Schrijvers DM, Lion E, et al. Poly(I:C) as cancer vaccine adjuvant: knocking on the door of medical breakthroughs. Pharmacol Ther. 2015;146:120–31.
13. Chuang JH, Lin TK, Tai MH, Liou CW, Huang ST, Wu CL, et al. Preferential involvement of mitochondria in toll-like receptor 3 agonist-induced neuroblastoma cell apoptosis, but not in inhibition of cell growth. Apoptosis. 2012;17:335–48.
14. Hsu WM, Hsieh FJ, Jeng YM, Kuo ML, Tsao PN, Lee H, et al. GRP78 expression correlates with histologic differentiation and favorable prognosis in neuroblastic tumors. Int J Cancer. 2005;113:920–7.
15. Chuang JH, Chuang HC, Huang CC, Wu CL, Du YY, Kung ML, et al. Differential toll-like receptor 3 (TLR3) expression and apoptotic response to TLR3 agonist in human neuroblastoma cells. J Biomed Sci. 2011;18:65.
16. Galli R, Paone A, Fabbri M, Zanesi N, Calore F, Cascione L, et al. Toll-like receptor 3 (TLR3) activation induces microRNA-dependent reexpression of functional RARbeta and tumor regression. Proc Natl Acad Sci USA. 2013;110:9812–7.
17. Bernardo AR, Cosgaya JM, Aranda A, Jimenez-Lara AM. Synergy between RA and TLR3 promotes type I IFN-dependent apoptosis through upregulation of TRAIL pathway in breast cancer cells. Cell Death Dis. 2013;4:e479.
18. Charakida A, Mouser PE, Chu AC. Safety and side effects of the acne drug, oral isotretinoin. Expert Opin Drug Saf. 2004;3:119–29.
19. Brelsford M, Beute TC. Preventing and managing the side effects of isotretinoin. Semin Cutan Med Surg. 2008;27:197–206.
20. Marabelle A, Sapin V, Rousseau R, Periquet B, Demeocq F, Kanold J. Hypercalcemia and 13-cis-retinoic acid in post-consolidation therapy of neuroblastoma. Pediatr Blood Cancer. 2009;52:280–3.
21. Cheung BB. Combination therapies improve the anticancer activities of retinoids in neuroblastoma. World J Clin Oncol. 2015;6:212–5.
22. Alvarez S, Germain P, Alvarez R, Rodriguez-Barrios F, Gronemeyer H, de Lera AR. Structure, function and modulation of retinoic acid receptor beta, a tumor suppressor. Int J Biochem Cell Biol. 2007;39:1406–15.
23. Cheung NK, Dyer MA. Neuroblastoma: developmental biology, cancer genomics and immunotherapy. Nat Rev Cancer. 2013;13:397–411.
24. Connolly RM, Nguyen NK, Sukumar S. Molecular pathways: current role and future directions of the retinoic acid pathway in cancer prevention and treatment. Clin Cancer Res. 2013;19:1651–9.
25. Arrieta O, Gonzalez-De la Rosa CH, Arechaga-Ocampo E, Villanueva-Rodriguez G, Ceron-Lizarraga TL, Martinez-Barrera L, et al. Randomized phase II trial of All-trans-retinoic acid with chemotherapy based on paclitaxel and cisplatin as first-line treatment in patients with advanced non-small-cell lung cancer. J Clin Oncol. 2010;28:3463–71.
26. Yu AL, Gilman AL, Ozkaynak MF, London WB, Kreissman SG, Chen HX, et al. Anti-GD2 antibody with GM-CSF, interleukin-2, and isotretinoin for neuroblastoma. N Engl J Med. 2010;363:1324–34.
27. Thiele CJ, Reynolds CP, Israel MA. Decreased expression of N-myc precedes retinoic acid-induced morphological differentiation of human neuroblastoma. Nature. 1985;313:404–6.
28. Silvis AM, McCormick ML, Spitz DR, Kiningham KK. Redox balance influences differentiation status of neuroblastoma in the presence of all-trans retinoic acid. Redox Biol. 2016;7:88–96.
29. Qiao J, Paul P, Lee S, Qiao L, Josifi E, Tiao JR, et al. PI3K/AKT and ERK regulate retinoic acid-induced neuroblastoma cellular differentiation. Biochem Biophys Res Commun. 2012;424:421–6.
30. Al Tanoury Z, Piskunov A, Rochette-Egly C. Vitamin A and retinoid signaling: genomic and nongenomic effects. J Lipid Res. 2013;54:1761–75.
31. Zaizen Y, Taniguchi S, Suita S. The role of cellular motility in the invasion of human neuroblastoma cells with or without N-myc amplification and expression. J Pediatr Surg. 1998;33:1765–70.
32. Sidell N, Rieber P, Golub SH. Immunological aspects of retinoids in humans. I. Analysis of retinoic acid enhancement of thymocyte responses to PHA. Cell Immunol. 1984;87:118–25.
33. Sidell N, Famatiga E, Golub SH. Immunological aspects of retinoids in humans. II. Retinoic acid enhances induction of hemolytic plaque-forming cells. Cell Immunol. 1984;88:374–81.
34. Kyi C, Roudko V, Sabado R, Saenger Y, Loging W, Mandeli J, et al. Therapeutic immune modulation against solid cancers with intratumoral poly-ICLC: a pilot trial. Clin Cancer Res. 2018;24:4937–48.
35. Helson L, Helson C. Human neuroblastoma cells and 13-cis-retinoic acid. J Neurooncol. 1985;3:39–41.
36. Shah N, Wang J, Selich-Anderson J, Graham G, Siddiqui H, Li X, et al. PBX1 is a favorable prognostic biomarker as it modulates 13-cis retinoic acid-mediated differentiation in neuroblastoma. Clin Cancer Res. 2014;20:4400–12.
37. Kohler JA, Imeson J, Ellershaw C, Lie SO. A randomized trial of 13-Cis retinoic acid in children with advanced neuroblastoma after high-dose therapy. Br J Cancer. 2000;83:1124–7.
38. Matthay KK, Villablanca JG, Seeger RC, Stram DO, Harris RE, Ramsay NK, et al. Treatment of high-risk neuroblastoma with intensive chemotherapy, radiotherapy, autologous bone marrow transplantation, and 13-cis-retinoic acid. Children's Cancer Group. N Engl J Med. 1999;341:1165–73.
39. Veal GJ, Cole M, Errington J, Pearson AD, Foot AB, Whyman G, et al. Pharmacokinetics and metabolism of 13-cis-retinoic acid (isotretinoin) in children with high-risk neuroblastoma—a study of the United Kingdom Children's Cancer Study Group. Br J Cancer. 2007;96:424–31.
40. Jacobs JL, Coyne CB. Mechanisms of MAVS regulation at the mitochondrial membrane. J Mol Biol. 2013;425:5009–19.
41. Flamini MI, Gauna GV, Sottile ML, Nadin BS, Sanchez AM, Vargas-Roig LM. Retinoic acid reduces migration of human breast cancer cells: role of retinoic acid receptor beta. J Cell Mol Med. 2014;18:1113–23.
42. Sidell N, Altman A, Haussler MR, Seeger RC. Effects of retinoic acid (RA) on the growth and phenotypic expression of several human neuroblastoma cell lines. Exp Cell Res. 1983;148:21–30.
43. Hertwig F, Peifer M, Fischer M. Telomere maintenance is pivotal for high-risk neuroblastoma. Cell Cycle. 2016;15:311–2.
44. Chou A, Itchins M, de Reuver PR, Arena J, Clarkson A, Sheen A, et al. ATRX loss is an independent predictor of poor survival in pancreatic neuroendocrine tumors. Hum Pathol. 2018;82:249–57.